Towards ML-ready hybrid solvers for wave–structure interaction: stability of loosely coupled floating system solvers

Bonaventura Tagliafierro & Malin Göteman

Dept. of Electrical Engineering, Uppsala University, Uppsala, Sweden
bonaventura.tagliafierro@angstrom.uu.se

HIGHLIGHTS

We propose a stability diagnostic for partitioning hydrodynamic forces to be used in hybrid solvers, enabling safe integration of linear components while directing machine learning (ML) to capture only the nonlinear, history-dependent force components.

1 INTRODUCTION

Hybrid solvers consist of procedures where the system dynamics is advanced in time using a combination of numerical models and machine learning (ML) components. For the integration of the motion of a rigid body interacting with water waves, data-driven force predictors may introduce stability issues when embedded in such solvers due to the force components that they surrogate. The coupling between fluid and structural domains can be addressed through various numerical strategies, ranging from monolithic approaches that solve both domains simultaneously within a unified framework, to partitioned methods that operate alternate leap-frog solutions between separate fluid and structural solvers with iterative exchange of boundary conditions [1]. In hybrid solvers, a neural network can replace or augment parts of the fluid solver, providing force predictions based on learned mappings from input features to hydrodynamic loads. A neural network can be compactly represented as:

$$\mathcal{N}_{\boldsymbol{\theta}}(\mathbf{x}) \equiv f(\mathbf{x};\boldsymbol{\theta}), \tag{1}$$

where $\mathbf{x}$ denotes the input features (e.g., kinematic quantities or flow parameters) and $\boldsymbol{\theta}$ the set of all trainable weights and biases. In the following, we will show how to select data to train a neural network of choice based on a stability criterion for numerical integration.

2 METHOD

In a fully coupled two-way wave–structure interaction, the fluid force F depends on the instantaneous state of the structure. Conversely, weakly coupled or one-way approaches, where fluid forces are prescribed with very weak or non-existent feedback from structural motion, may introduce stability issues when the implicit damping characteristics of the prescribed forces are small or negative. This can be formulated starting from:

$$m\ddot{z}_{ref} = F_{\text{total}}(t) \tag{2}$$

where $F_{\text{total}}(t)$ is a predetermined function of time only, which may be considered as generated from a one-way coupling, computational method measurements, or experimental reverse dynamics (i.e., black boxes). Also, the body dynamics is fully known.

We assume that this black-box force can be decomposed into known and unknown components:

$$F_{\text{total}}(t) = F_{\text{known}}(z, \dot{z}, \ddot{z}) + F_{\text{bb}}(t), \tag{3}$$

where F_{known} includes explicitly modeled physics such as hydrostatic restoring forces, added mass effects, and damping, which can be related to system dynamics, while $F_{\text{bb}}(t)$ represents the prescribed

fluid force from simulations or experiments. The reconstruction reads:

$$m\ddot{z} = F_{\text{known}}(z, \dot{z}, \ddot{z}) + F_{\text{bb}}(t). \tag{4}$$

The reference trajectory can be reconstructed by numerically integrating this system with appropriate initial conditions z_0 and $\dot{z}_0$. This integration yields the time histories $z(t)$ and $\dot{z}(t)$ that should correspond to the reference motion. To assess the stability of this reconstructed system, we extract the implicit characteristics of the prescribed force by regressing F_{bb} against the reference motion. This force is decomposed into components proportional to velocity, displacement, and acceleration:

$$F_{\text{bb}}(t) \approx \bar{F} + \alpha\ddot{z}_{\text{ref}}(t) + \beta\dot{z}_{\text{ref}}(t) + \gamma z_{\text{ref}}(t), \tag{5}$$

where $\bar{F}$ is the mean force, $\alpha = \partial F_{\text{bb}}/\partial\ddot{z}|_{\text{ref}}$, $\beta = \partial F_{\text{bb}}/\partial\dot{z}|_{\text{ref}}$, and $\gamma = \partial F_{\text{bb}}/\partial z|_{\text{ref}}$ are the force sensitivities to velocity and displacement, respectively. These coefficients are obtained through least-squares regression:

$$\begin{bmatrix}\alpha\\ \beta\\ \gamma\end{bmatrix} = \left(\mathbf{A}^T\mathbf{A}\right)^{-1}\mathbf{A}^T\left(F_{\text{bb}} - \bar{F}\right), \tag{6}$$

with the regression matrix defined as:

$$\mathbf{A} = \begin{bmatrix}\ddot{z}_{\text{ref}}(t_1) & \dot{z}_{\text{ref}}(t_1) & z_{\text{ref}}(t_1)\\ \vdots & \vdots & \vdots\\ \ddot{z}_{\text{ref}}(t_N) & \dot{z}_{\text{ref}}(t_N) & z_{\text{ref}}(t_N)\end{bmatrix}. \tag{7}$$

where $1 \dots N$ iterates the time instances in the investigated time history.

To interpret these coefficients in the context of the structural dynamics, we rewrite Equation 4 by substituting Equation 5:

$$m\ddot{z} = F_{\text{known}}(z, \dot{z}, \ddot{z}) + \bar{F} + \alpha\ddot{z} + \beta\dot{z} + \gamma z. \tag{8}$$

These regression coefficients α, β, and γ directly specify the mass, damping, and stiffness required in the ODE solver to achieve stable integration. This information can then be used to decide whether a component can be part of the integration system, according to the required compensation.

2 APPLICATION FRAMEWORK

To evaluate the proposed approach, two numerical models are employed to generate pseudo time histories of the black-box force F_{bb}. The first model is based on hydrodynamic forces obtained from a frequency-domain boundary element method (BEM) solver. Linear hydrodynamic coefficients are used to solve the system dynamics in the time domain. The corresponding equation of motion is given by:

$$(m + A_\infty)\ddot{z}(t) + \int_0^t K(t-\tau)\dot{z}(\tau)d\tau + Cz(t) = F_e\,, \tag{9}$$

where, m is the inertial mass, A_∞ is the added mass associated with heave mode, $K(t)$ is the convolution part of the radiation force, C is the hydrostatic stiffness, and F_e is an external force. The linear coefficients are found using the frequency-domain BEM library Capytaine [2] considering a perfectly half-submerged sphere located at rest at its statically neutrally buoyant position. The radiation damping term is calculated using:

$$K(t) = \frac{2}{\pi}\int_0^\infty B(\omega)\cos(\omega t)d\omega\,, \tag{10}$$

where $B(\omega)$ is the radiation damping computed by the BEM solver. The main parameters for this model are: m=7.06 kg; A_∞=3.50 kg; C=692.2 N/m.

Secondly, a high-fidelity fluid dynamics solver is employed, based on the direct solution of the Navier–Stokes equations. The flow evolution is computed by interpolating physical quantities over neighboring particles, following a Lagrangian formulation. The governing equations for transient compressible flows consist of the conservation of mass and momentum, which in Lagrangian form can be written as:

$$\frac{d\rho}{dt} + \rho\nabla\cdot\mathbf{v} = 0, \qquad \text{and} \qquad \frac{d\mathbf{v}}{dt} = -\frac{1}{\rho}\nabla p + \nu\triangle\,\mathbf{v} + \mathbf{f}\,, \tag{11}$$

where ρ, t, $\mathbf{v}$, p, ν and $\mathbf{f}$ are density, time, velocity vector, pressure, kinematic viscosity, and external forces per unit mass, respectively. Numerically, this system of equations is solved using the smoothed particle hydrodynamics method (SPH), employing an open-source implementation [3].

Figure 1 presents validation for both numerical models against experimental data available in [4]. The test case comes from a heavy decay test of a half-submerged sphere of diameter D with an initial drop height of $D/10$. The BEM model mesh for the computation of the hydrodynamic parameters consists of 6400 panels, and it is resolved for 400 frequencies, log-spaced between 0.10 rad/s and 40.0 rad/s. SPH is initialized with a cartesian lattice evenly spaced at Δp of $D/20$, yielding a total of 12M particles for fluid and boundary particles.

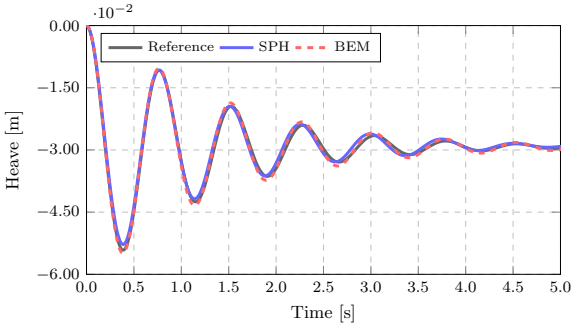

Figure 1: Validation for the two numerical models against experimental data.

2.1 Analysis

The models validated above are utilized to resolve the dynamics of the sphere under monochromatic waves of period T=0.75 s and wave height H=0.05 m; this frequency is chosen very close to the resonance frequency of the system (T_e=0.76 s). For the linear potential flow method (here labeled "BEM"), the excitation force (F_e) is determined as a sinusoidal function, whereas in the SPH based model, monochromatic waves are generated using a wavemaker. Thus, the output of the two models constitutes the starting point to analyze the decomposition of the total fluid forces as measured. The outputs of the regression analysis are reported in Table 1, whereas the system dynamics recovered from the integration of the system for the three cases is shown in Figure 2.

Table 1: Force sensitivity coefficients from regression $F_{\text{bb}} \approx \bar{F} + \alpha\ddot{z} + \beta\dot{z} + \gamma z$.

		BEM			SPH		
Case	F_{bb}	α [kg]	β [Ns/m]	γ [N/m]	α [kg]	β [Ns/m]	γ [N/m]
1	F_{tot}	7.06	0.00	0.0	7.06	0.00	0.0
2	$F_{\text{tot}} - Cz_{\text{ref}}$	7.06	0.00	692.2	7.06	0.00	692.2
3	$F_{\text{tot}} - Cz_{\text{ref}} - A_\infty\ddot{z}_{\text{ref}}$	10.56	-0.04	692.5	7.85	0.12	503.3

For Case 1, the regression of the total force yields $\beta \approx 0$ and $\gamma \approx 0$ for both BEM and SPH, with only the mass term coefficient $\alpha = 7.06$ kg being fully compliant with the inertial mass. This result is expected: as the reference motion was generated by integrating these same forces, the damping and stiffness contributions are inherently balanced, leaving no net sensitivity to velocity or displacement. To reconstruct this motion, the ODE solver requires no explicit damping or stiffness,

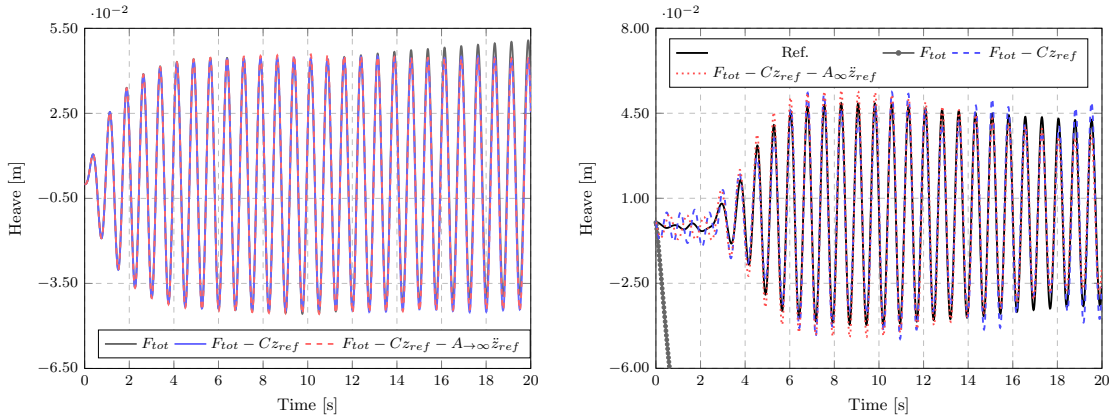

Figure 2: Heave motion evolution for the BEM (left) and SPH (right) as reconstructed for a sphere subject to monochromatic waves of period T=0.75 s and wave height H=0.05 m.

resulting in a neutrally stable system that can drift under perturbations. This is evidenced by the integration output in Figure 2, where the two models present some drift. For the SPH, this instability is exacerbated by an intrinsic spatial discretization error between boundary and fluid.

When the hydrostatic restoring force is taken out in Case 2, it reveals $\gamma = 692.2$ N/m for both methods (corresponding to the modeled one), indicating that the remaining force has a positive correlation with displacement. Rather than implying instability per se, this indicates that the ODE solver needs to include a stiffness value to compensate for the removed component. With this stiffness in place, the system gives good accuracy for both, with SPH suffering from some inaccuracies. However, extra damping can benefit both stability and accuracy. Removing the infinite-frequency added mass for Case 3, it exposes differences between BEM and SPH output models. BEM yields a small stabilizing contribution with perfect agreement for total mass and stiffness, while SPH shows a destabilizing tendency, and modified physical mass coefficients and stiffness. This is reflected by inaccuracies in the time series in Figure 2.

3 OUTLOOK

For the final presentation of this work, we intend to show an application of this method to the selection of hydrodynamic components for floating structure simulations, and present a preliminary overview of the envisioned hybrid solver comprising a feed-forward neural network for force prediction. Concluding, an application for a floating offshore wind platform will be presented.

REFERENCES

[1] Benra, F.-K., Dohmen, H. J., Pei, J., Schuster, S., and Wan, B. 2011. *A Comparison of One-Way and Two-Way Coupling Methods for Numerical Analysis of Fluid-Structure Interactions.* Journal of Applied Mathematics 2011(1), 853560.

[2] Ancellin, M., and Dias, F. apr 2019. *Capytaine: a Python-based linear potential flow solver.* Journal of Open Source Software 4(36), 1341.

[3] Domínguez, J. M., Fourtakas, G., Altomare, C., Canelas, R. B., Tafuni, A., García-Feal, O., Martínez-Estévez, I., Mokos, A., Vacondio, R., Crespo, A. J. C., Rogers, B. D., Stansby, P. K., and Gómez-Gesteira, M. September 2022. *DualSPHysics: from fluid dynamics to multiphysics problems.* Computational Particle Mechanics 9(5), 867–895.

[4] Kramer, M. B., Andersen, J., Thomas, S., Bendixen, F. B., Bingham, H., Read, R., Holk, N., Ransley, E., Brown, S., Yu, Y.-H., Tran, T. T., Davidson, J., Horvath, C., Janson, C.-E., Nielsen, K., and Eskilsson, C. 2021. *Highly Accurate Experimental Heave Decay Tests with a Floating Sphere: A Public Benchmark Dataset for Model Validation of Fluid–Structure Interaction.* Energies 14(2).